Micellization in Block Polyelectrolyte Solutions. 3. Static Light Scattering Characterization

Karine Khougaz, Irina Astafieva,† and Adi Eisenberg*

Department of Chemistry, McGill University, 801 Sherbrooke Street West, Montréal, Québec, Canada H3A 2K6

Received January 13, 1995; Revised Manuscript Received June 13, 1995®

ABSTRACT: Block polyelectrolyte micelles formed by poly(styrene-*b*-sodium acrylate) in aqueous solutions were characterized by static light scattering (SLS). Initially, the solutions contained gel-like particles; the kinetics of disentanglement of these particles were measured from the intensity of the scattered light at different angles as a function of heating time at 100 °C. It was found that after ca. 50 h of heating no further changes occurred in the scattered intensity. The effect of different sodium chloride concentrations on the aggregation numbers (N), radii of gyration (R_g), and second virial coefficients (A_2) of the resulting micellar solutions was determined for two block copolymers, PS(6)-*b*-PANa(180) and PS(23)-*b*-PANa-(300). It was found that N increased as a function of salt concentration at low salt contents, but the values remained constant above ca. 0.10 M NaCl. A range of samples with PS block lengths ranging from 6 to 71 units and PANa block lengths ranging from 44 to 780 units was measured in 2.5 M NaCl. As expected, the length of the insoluble block had a much greater effect on the aggregation numbers than that of the soluble block. The data were examined according to the scaling predictions of the star model and several mean-field models. Comparison with several of the models showed good agreement with experimental values of N, calculated core radius (R_c), and R_g as a function of block lengths. The core radii values of the micelles agreed very well with those determined independently for similar samples measured in the solid state by small-angle X-ray scattering (SAXS). From this result, it was concluded that the micelles in 2.5 M NaCl exist singly, i.e., that no supermicellar aggregates are present and that the core is solvent free.

1. Introduction

Considerable interest has recently focused on micelles formed by block copolymers.[1−5] With the advances made in the synthesis of block copolymers by anionic polymerization, specific tailored systems can be created for use in applications such as drug delivery[6] and catalysis.[7] An understanding of the relation between the physical properties of the block copolymer micelles, such as their critical micelle concentration (cmc), size, molecular weight, and behavior in different media, and their structure not only is of academic interest but also is very important for such applications.

In the preceding two papers of this series, the micellization of a block polyelectrolyte system, poly(styrene-*b*-sodium acrylate) (PS-*b*-PANa), was investigated.[8,9] The cmc values of this system were determined from fluorescence measurements for a range of block polyelectrolyte samples. It was found that an increase in the insoluble PS block length lowered the cmc; for example, when the PS block length increased from 6 to 110 units, the cmc decreased from 1.6×10^{-5} to 5×10^{-8} M.[8] An increase in the length of the soluble PANa block had a weaker effect on the cmc. The second paper, directly preceding this one, further explored the effects of the PANa block length and the effect of salt on the cmc values.[9] A maximum was observed in the cmc at short PANa block lengths; this maximum was ascribed to the balance between an increase in solubility with increasing block length for short blocks and a subsequent decrease in solubility with further increase in the PANa block length. The cmc was also investigated in the range of 0.10−2.5 M NaCl concentrations, and, for most of the samples, the cmc decreased linearly with the square root of the salt concentration.

In the previous publication,[8] it was shown that the intrinsic viscosity of block polyelectrolyte solutions depends strongly on the thermal history of the samples, i.e., on the time and temperature of sample storage. It was found that heating a block polyelectrolyte solution of PS(40)-*b*-PANa(520) at 100 °C for ca. 80 h yielded a solution in which the viscosity was no longer dependent on further heating. The cmc values as determined by fluorescence spectroscopy showed no difference for samples which were heated or unheated. This latter result implies that micelle-like structures are present in both the unheated and heated solutions. The decrease in viscosity was attributed to the disruption of supermolecular aggregates which exist as a result of entanglements in the polyelectrolyte chains. The reader is referred to the first paper of this series for a survey of previous work pertaining to block copolymer micelles.[8] The second paper reviews the recent work concerning block polyelectrolyte micelles as well as the relevant theories regarding polyelectrolytes and polyelectrolyte micelles.[9] For convenience, in this section, only a very brief review of the theories related to block polyelectrolyte micelles will be given.

There are many models dealing with the structure of polymeric micelles.[5] Some of these models has been applied to polymeric micelles, and good agreement with experiments have been observed.[10−12] In general, the models can be categorized into two groups, the mean-field models[13−18] and the star models.[19,20] The first describes micelles which are composed of a large core and a relatively thin and dense corona. The micellar corona is treated as having a uniform density. In the star models, on the other hand, the corona density decreases with increasing distance from the core. The star model was first proposed by Daoud and Cotton to describe the conformation of star-shaped polymers.[21]

* Author to whom correspondence should be addressed.
† Present address: Anergen Inc., 301 Penobscot Drive, Redwood City, CA 94063.
® Abstract published in *Advance ACS Abstracts,* September 1, 1995.

0024-9297/95/2228-7135$09.00/0

This model was later extended by Zhulina and Birshtein where scaling relations for the micellar characteristics were determined depending on the copolymer composition.[19] In this model, four regions were distinguished, depending on the relative lengths of the block forming the core (N_B) and that forming the corona (N_A). Halperin[20] also extended the model of star-shaped polymers and, for the case when $N_B \ll N_A$, obtained scaling relations which agreed with those of Zhulina and Birshtein.[19] From a minimization of the free energy of the system, scaling predictions for the aggregation numbers and core and micelle radii were given as a function of the block lengths in these two theories.

There are two specific theories describing the micellization of block polyelectrolytes in solution, that of Marko and Rabin[22] and that of Dan and Tirrell.[23] The first theory describes micelle formation in the weak and in the strong charge limit. The theory by Dan and Tirrell investigates the aggregation properties of these micelles in aqueous salt solutions. For moderate salt concentrations, the scaling relations accounting for the polyelectrolyte nature of the corona were found to be the same as those predicted for micelles of neutral diblocks in a highly selective nonpolar solvent.[20,24] Therefore, the aggregation number, cmc, and chemical potential of block polyelectrolyte micelles are dominated by the core block. It should be noted that there are also several theories describing the properties of polyelectrolytes attached to surfaces.[25,26] For example, Ronis describes the conformations of the polyelectrolyte block attached to a spherical surface as a function of several parameters, such as the screening length, the curvature of the colloid core, and the number of chains emanating from the core.[26]

The purpose of the present paper is to characterize the block polyelectrolyte micelle system, poly(styrene-*b*-sodium acrylate), by SLS. First, the kinetics of disentanglement of the block copolymers in aqueous solutions will be investigated as a function of different heating periods for several samples. Second, the effect of salt concentration on the micellar characteristics will be examined. Third, the micelles formed from a wide range of samples with PS lengths ranging from 6 to 71 units and PANa lengths ranging from 44 to 780 units will be characterized in 2.5 M NaCl. Theoretical scaling models will then be applied to investigate the agreement with the results obtained for these micelles which were formed under nonequilibrium conditions. In the final section, comparisons to results obtained on similar samples from the solid state as well as to literature values for poly(styrene-*b*-ethylene oxide) (PS-*b*-PEO) micelles in water will be presented.

2. Experimental Section

2.1. Materials. The reader is referred to the preceding paper in this series for information pertaining to the synthesis of the block copolymers.[8] The sample notation used indicates the copolymer composition; for example, PS(23)-*b*-PANa(44) represents a polystyrene chain of 23 units joined to a poly(sodium acrylate) chain of 44 units.

2.2. Sample Preparation for Static Light Scattering (SLS). The polymer samples for the SLS measurement were dissolved in deionized water (Millipore MILLI-Q) and heated at 100 °C for 5 days in sealed glass ampules. The concentration of the stock solutions was ca. 1−3 mg/mL. These solutions were diluted with the appropriate amount of sodium chloride (NaCl, 99.999%, Aldrich) solutions to obtain polymer solutions of the required salt concentration and stirred overnight. The aqueous salt solutions were filtered through filters of 0.22 μm pore size, and the polymer solutions were filtered through filters of either 0.45 or 0.8 μm pore size, depending on the composition of the block copolymer. In general, for the block copolymers with polystyrene lengths ranging from 6 to 40 units, the 0.45 μm filter was used when the poly(sodium acrylate) chain length was below 300 units, and the 0.80 μm filter was employed in all other cases. The filters used were always rinsed first with 10 mL of solvent prior to solvent and sample filtration in order to remove any possible contaminants. A common problem with the clarification of polyelectrolytes is polymer retention on the filters. Thus, as a precaution, the filter was rinsed with 4 mL of sample solution prior to sample filtration, which would saturate any possible adsorption sites on the filter. Also, the filter membrane was composed of cellulose acetate which showed negligible polymer retention.

The kinetics of micelle disentanglement was studied by dissolving the polymers in 0.10 M NaCl solutions and stirring overnight at room temperature. The solutions were then sealed, and the scattered intensity was measured at room temperature as a function of heating time at 100 °C. Two different procedures were used for this measurement. In the first method, different solutions of approximately the same concentration were transferred into separate ampules which were then sealed, heated, and opened after different heating times. The solutions were then filtered into the scintillation vials for the light scattering measurement once the solutions reached room temperature. The second method involved filtering the unheated solutions into scintillation vials which were then sealed and heated. The solutions were then removed, cooled, measured, and reheated without breaking the seal.

2.3. SLS Measurement. Light scattering experiments were performed using a DAWN-F multiangle laser photometer (Wyatt Technology, Santa Barbara, CA) at 25 °C, which operates at 15 angles, from 26 to 137°, and is equipped with a He−Ne laser (632.8 nm). Data acquisition and analysis utilized DawnF and SkorF software, respectively. The polymer solutions were filtered directly into scintillation vials, which were used for the light scattering measurements. The measurement was performed by dilution of a stock solution which had an approximate concentration in the range of 1×10^{-3}−2×10^{-5} g/mL, depending on the molecular weight of the sample; the concentrations were always larger than the cmc values as determined previously by fluorescence measurements.[9] A minimum of four concentrations were used to determine the weight-average molecular weight, radius of gyration, and second virial coefficient with the aid of either a Zimm or a Debye plot, processed with the Aurora software.

2.4. Specific Refractive Index Increment Measurement (d*n*/d*c*). The specific refractive index increment (d*n*/d*c*) was determined using the Wyatt/Optilab 903 interferometric refractometer and accompanying software (Dndc 2.01) at a wavelength of 630 nm. The cell constant was determined by calibration with different concentrations of sodium chloride (99.999%, Aldrich) solutions. Eight to ten concentrations were measured for each d*n*/d*c* determination. For the polymers measured in salt solutions, the sample solutions were dialyzed exhaustively for 1 week in dialysis membranes with a molecular weight cutoff of either 8000 or 15 000 against the appropriate salt concentration. Prior to measurement, the dialysate was filtered and used in the reference cell. The d*n*/d*c* values were determined from the slope of a plot of refractive index versus polymer concentration. The polymer concentrations before and after dialysis were monitored by measuring the scattered intensity at 90°; the concentrations were found to deviate by as much as 10% for some samples.

3. Results and Discussion

The Results and Discussion part is divided into six sections. In the first section, SLS theory and data manipulation will be described. The second section will address the kinetics of disentanglement of the micelles in solution for different heating times. The third and fourth sections will address the SLS results of the block polyelectrolyte micelles as a function of salt concentra-

tions and, in more detail, at one constant salt concentration, i.e., 2.5 M NaCl, respectively. Applications of scaling theories will be given in section 5. In the final section, comparisons will be made with solid-state results of the same system and with the aqueous nonionic micelle system PS-*b*-PEO.

3.1. Theory

Static light scattering is a convenient method of characterizing polymer solutions which gives the weight-average molecular weight, radius of gyration, and virial coefficients. When the particle size is greater than approximately $\lambda/20$, it has been shown that[27]

$$Kc/R(\theta) = \frac{1}{P(\theta)\,M_w} + 2A_2c + \ldots \quad (1)$$

where K is the optical constant $(2\pi^2(n\ dn/dc)^2/\lambda_0^4 N_{Av})$, n is the refractive index of the solvent, dn/dc is the specific refractive index increment, λ_0 is the wavelength in vacuum, N_{Av} is Avogadro's number, c is the concentration, $R(\theta)$ is the Rayleigh ratio at the angle of measurement, $P(\theta)$ is the particle scattering function, M_w is the weight-average molecular weight, and A_2 is the second virial coefficient; since the solutions are dilute, the higher order virial coefficients have been neglected.

The particle scattering function describes the angular variation of the scattered intensity and accounts for the intraparticle interference. It can be expressed in the form of a power series in $\sin(\theta/2)$,

$$P(\theta) = 1 - \alpha_1 \sin^2(\theta/2) + \alpha_2 \sin^4(\theta/2) - \ldots \quad (2)$$

For small angles of observation, the reciprocal scattering function is given by

$$P(\theta)^{-1} = 1 + \frac{16\pi^2}{3\lambda^2}\langle R_g^2\rangle_z \sin^2(\theta/2) \quad (3)$$

where $\langle R_g^2\rangle_z$ is the square z-average radius of gyration. Therefore, from the initial slope of the inverse particle scattering function as a function of $\sin^2(\theta/2)$, the particle size can be evaluated independent of the particle shape.

A graphical method used to solve eq 1, with the particle scattering function given by eq 3, was developed by Zimm.[28] By plotting $Kc/R(\theta)$ for different angles and concentrations as a function of $\sin^2(\theta/2) + kc$, where k is a scaling factor, and extrapolating to zero concentration, information on the particle size can be obtained from the initial linear slope (eq 3). Similarly, in the limit of $\theta \to 0$, the particle scattering function is equal to unity, and the slope of the line is proportional to the second virial coefficient. The intercepts from the zero concentration and zero angle lines yield the inverse weight-average molecular weight. This graphical double linear extrapolation method is referred to as a Zimm plot.[28]

For particles of very high molecular weight (e.g., $>10^6$ g/mol), $Kc/R(\theta)$ exhibits significant curvature in the angular dependence. In these cases, special care must be taken when analyzing the data.[29] It should be noted that, for these high molecular weight cases, small errors in the extrapolations can result in a relatively large error when the reciprocal is computed in the Zimm plot for the evaluation of the molecular weight. Similarly, there would be a large error in the radius of gyration which depends on the M_w value. In these cases, the Debye plot, which is similar to the Zimm plot with the exception that the ordinate is plotted as $R(\theta)/Kc$, can be used. In the present study, both the Zimm and Debye plots were employed; their specific applications to the different block polyelectrolyte systems are discussed in section 3.3.2.

A second problem in the analysis of large particles is the evaluation of the radius of gyration from the angular dependence. The Zimm method is based on linear extrapolations of the concentrations and the angles. However, for large particles, the angular dependence is nonlinear at high angles. Thus, the data which depart significantly from linearity should be omitted in the analysis.[29] The advantage of the present instrument is the accessibility of a wide range of angles. Thus, it is possible to fit the angular dependence with a polynomial expansion of the particle scattering function in which the term linear in $\sin^2(\theta/2)$ would yield the radius of gyration (R_g) (eq 2). The comparison of the R_g values determined by these two methods will be given in section 3.4.3.

The dissymmetry in the light scattered from large particles can be evaluated from the dissymmetry ratio, Z_d. This quantity is defined as the ratio of the scattered light of two angles which are symmetric about 90°. Most frequently, the angles used are 45° and 135°,

$$Z_d = \frac{P(45)}{P(135)} = \frac{R(45)}{R(135)} \quad (4)$$

This quantity is a measure of the particle size, since, for large particles, the scattering at low angles will be larger due to constructive interference of the scattered light from the particle. Also, the scattering at large angles will be reduced due to destructive interference of the scattered light. These dissymmetry ratios can also be correlated to various particle shapes.

Polyelectrolyte solutions with added salt are multicomponent systems consisting of polyions, co-ions, and counterions. The above theory can be used for these systems if the specific refractive index increment values are determined at constant chemical potential.[30] These values are determined after establishing Donnan equilibrium between the polyelectrolyte solution and the solvent by dialysis. Also, it should be noted that for block copolymers, due to the compositional heterogeneity of the systems, the M_w, R_g, and A_2 values refer to apparent values.[27]

Micellar parameters can be calculated from the value of the apparent M_w. For instance, the aggregation numbers (N) for block copolymer micelles are evaluated from the ratio of the apparent M_w of the micelles to that of the unassociated polymer. The core radius (R_c) can be calculated from N using the following relation for the core volume, V_c,

$$V_c = (4/3)\pi R_c^3 = N N_B M/\varrho N_{Av} \quad (5)$$

where N_B, M, and ϱ are the number of repeat units, the repeat unit molecular weight, and the density (1.05 g/mL)[31] of the PS block, respectively. From the R_c values and N it is possible to evaluate the surface area per chain (S/N), given as

$$S/N = 4\pi R_c^2/N \quad (6)$$

3.2. Time Dependence of SLS Data—Kinetics of Disentanglement. In a previous viscometric study, it

was found that the PS-*b*-PANa samples in water form supermolecular aggregates which disaggregate upon heating.[8] The present study by SLS was performed in order to supplement the previous results and to give further insight into this process. Initially, under the preparation conditions used here, the solid-state morphology of PS-*b*-PANa samples, which were recovered by freeze drying, consisted of a collapsed PS core surrounded by a matrix consisting of PANa chains. For the present block copolymer system, dissolution of the block copolymer may involve first the penetration of water into the continuous polyelectrolyte matrix, which, because of the slow dissolution of the PANa, would result in the formation of nonuniform gel-like particles. Indeed, it was observed that samples prepared at a concentration of, for example, 3 mg/mL formed initially a nonuniform gel-like phase. These gel-like structures were more prevalent in block polyelectrolytes which had long PANa block lengths, e.g., 300 units. Upon heating, the interpenetrating ionic domains begin to dissociate, and the gel-like structures dissolve. It is interesting to note that the formation of a nonuniform gel phase was also apparent in poly(sodium acrylate) homopolymer prior to heating. Also, metastable structures have been found to exist in other micellar systems such as poly(styrene-*b*-ethylene-*co*-propylene) (PS-*b*-PEP) in decane.[32] It has been postulated that these structures arise from the solid-state morphology.

In the present study of the disaggregation process, the solutions employed should be in the dilute concentration regime, whether the chains are present as single chains or as micelles. This regime has been defined[33,34] as being below the overlap concentration, c^*, where

$$c^* = M/N_{Av}R_g^3 \qquad (7)$$

where M is the molar mass. For example, for a typical block copolymer, PS(23)-*b*-PANa(300), with a number-average molecular weight (M_n) of 3×10^4 and a radius of gyration of ca. 30 nm, the overlap concentration is ca. 2 mg/mL. For the micelle of a molecular weight of 5×10^6 and a R_g of 100 nm, the overlap concentration is ca. 8 mg/mL. These concentrations show that the SLS studies were performed in the dilute solution regime, and therefore the physical processes which occur at higher concentrations should not be operative. For instance, in the semidilute region, pseudogel domains are found; i.e., entangled polymer solutions behave as polymer networks swollen by the solvent. However, the gel-like phase, which could be present because of incomplete disentanglement of the ionic domains, as described earlier, may be present at a microscopic level in dilute solutions.

In order to determine meaningful aggregation numbers and micelle sizes by SLS, one should be sure that single micelles and not supermolecular aggregates are present in solution. Thus, a study of the kinetics of disentanglement was performed by static light scattering to supplement the previous viscosity study. SLS is a convenient method for this study, since information on the size and molecular weight of the particles in solution can be obtained from the angular dependence of the scattered light and from the magnitude of the scattered intensity, respectively.

Two methods of sample preparation for the study of disentanglement were described previously in the Experimental Section. The first method involved heating several separate solutions for different periods of time and filtering the solutions after a cooling period. The second method involved initial filtration of unheated solutions into vials, which were then sealed and subsequently used directly for the light scattering measurements. The disadvantage of the second method is that the solutions, prior to heating, were very difficult to filter; thus, it is likely that some of the supermicellar structures were removed by this process. In contrast, the solutions prepared by the first method were relatively easy to filter after a minimum amount of heating (1 h), so it seems reasonable to expect that no significant amount of supermolecular aggregates were removed. Also, it should be noted that in both cases it was found that the scattered intensity as a function of angle was independent of the cooling times and cooling methods, i.e., gradual cooling or rapid quenching to room temperature.

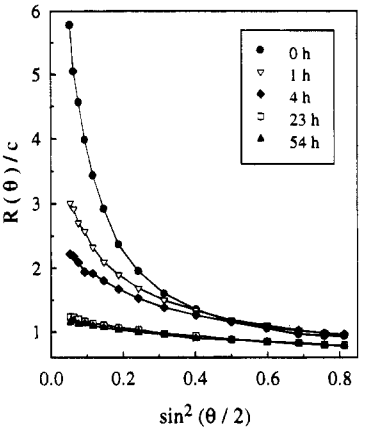

Figure 1. Effect of different heating times on the plot of the normalized Rayleigh ratio as a function of $\sin^2(\theta/2)$ for PS(40)-*b*-PANa(520).

Figure 1 shows the plots of the Rayleigh ratio as a function of angle, $\sin^2(\theta/2)$, for different heating periods at 100 °C for the PS(40)-*b*-PANa(520) system at a concentration of 6.8×10^{-5} g/mL. The solutions were prepared by the first method described, i.e., by heating, filtering, and measuring individual samples. It can be seen from this figure that the intensity of the scattered light at low angles decreases as a function of heating time, with the most significant changes occurring at low angles during the first 4 h. For instance, the dissymmetry ratios as defined by eq 4 for the unheated sample and those heated for 1, 4, and 23 h were 3.7, 2.4, 2.0, and 1.4, respectively. The decrease in the dissymmetry of scattered light with longer heating times shows the progressive disappearance of large particles which would scatter light considerably at low angles. For the longest heating period of 54 h, no significant further change in the Rayleigh ratios was observed. From this result, it can be concluded that most of the supermolecular aggregates have disentangled before ca. 50 h of heating. The SLS results are in qualitative agreement with the viscosity results for the same polymer sample reported previously.[8] For an incubation temperature of 100 °C, a plateau in the viscosity was attained after 80 h of heating. Also, the viscosity of the sample was found to decrease rapidly in the first few hours of heating and to decrease more gradually with longer heating times.

In the present case, it is important to understand how the molecular parameters of block polyelectrolytes, i.e., the PS and PANa block lengths, influence the kinetics of disentanglements. These studies were performed on

Table 1. Characterization of Poly(styrene-*b*-sodium acrylate) in 0.10 and 2.5 M NaCl by SLS for Different Heating Periods at 100 °C[a]

PS(*X*)-*b*-PANa(*Y*)	C_s (M)	$M_w \times 10^{-6}$	N	$R_g^{(a)}$ (nm)	$R_g^{(b)}$ (nm)	$A_2 \times 10^4$ (mL mol/g^2)	R_c (nm)	S/N (nm^2/chain)	Z_d
				1 day of Heating					
23-*b*-160	0.10	9.2	530	93		−0.060			1.6
86-*b*-190	0.10	30	1100	110		−0.098			1.8
				5 days of Heating					
6-*b*-89	0.10	0.48	54	78	61	0.32	2.4	1.2	1.7
	2.5	0.53	59	75	64	−1.2	2.4	1.2	1.7
6-*b*-180	0.10	0.43	24	46	34	0.87	1.8	1.6	1.2
	2.5	0.45	26	37	30	−0.20	1.8	1.6	1.2
6-*b*-400	0.10	0.60	16	40	36	2.8	1.6	1.8	1.2
	2.5	0.68	18	37	36	2.5	1.6	1.8	1.2
11-*b*-69	2.5	0.49	65	91	72	−0.96	3.0	1.8	1.4
11-*b*-160	2.5	1.0	63	64	55	0.27	3.0	1.8	1.3
11-*b*-350	2.5	2.7	79	92	82	2.5	3.3	1.7	1.5
23-*b*-44	2.5	0.92	140	30	30	−3.5	5.1	2.3	1.0
23-*b*-81	2.5	1.6	160	44	40	1.4	5.2	2.2	1.1
23-*b*-160	0.10	2.5	140	45	40	1.4	5.1	2.3	1.2
	2.5	2.6	150	51	40	−0.034	5.4	2.1	1.2
23-*b*-300	2.5	4.5	150	90	80	−0.36	5.1	2.2	1.7
23-*b*-780	2.5	19	250	140	130	−0.13	6.1	1.9	6.1
40-*b*-82	2.5	2.2	190	50	40	−0.69	6.7	3.0	1.1
50-*b*-89	2.5	5.0	370	34	30	−1.2	9.0	2.8	1.1
50-*b*-330	2.5	21	570	120	110	−0.46	10	2.4	3.0
71-*b*-120	2.5	5.5	290	71	57	0.44	9.4	3.8	1.2
86-*b*-190	0.10	18	550	55	50	−0.51	12	3.5	1.3

[a] The R_g values were evaluated in (a) from either a Debye or a Zimm plot and in (b) from linear extrapolations of Debye plots excluding higher angles. The calculations for N were done using three significant figures and subsequently rounded to two significant figures.

various block copolymers prepared by the second method, i.e., by heating and measuring the sample in one sealed ampule. Certain trends for micelle disentanglement were observed. First, for block copolymers composed of a short PS block of 23 units and a PANa block of 81 units, the equilibrium was established after 30 min, as observed by no further change in the magnitude of the Rayleigh ratio at different angles. In contrast, for a sample with the same PS block length but a longer PANa block length of 330 units, equilibration took 24 h. A similar trend was also observed for a PS block length (40 units), in that the samples with the longer PANa blocks reached equilibrium more slowly. This result is to be expected, since there would be more entanglements present with longer PANa units. The ratio of the Rayleigh ratio (90°) at $t = 0$ (no heating) and the Rayleigh ratio after a certain heating time, such as 20 h, were compared. The samples, in order of increasing equilibration time, were found to be in the order of PS(23)-*b*-PANa(81) ~ PS(11)-*b*-PANa(160) < PS(40)-*b*-PANa(180) < PS(23)-*b*-PANa(330) < PS(40)-*b*-PANa(520). Thus, the PANa block size seems to be the determining factor in the disentanglement of the supermolecular aggregates.

In order to obtain a quantitative measure of the dissociation of supermicellar structures, aggregation numbers were evaluated for block polymers subjected to heating times of 1 and 5 days in a 0.10 M NaCl salt concentration. The aggregation numbers are given in Table 1 for two samples, PS(23)-*b*-PANa(160) and PS(86)-*b*-PANa(190). For instance, for PS(23)-*b*-PANa(160), the aggregation numbers were 530 and 140, and for PS(86)-*b*-PANa(190), they were 1100 and 550, for heating periods of 1 day and 5 days, respectively. Similarly, the apparent radii of gyration for the two samples decreased to ca. half their size after 5 days of heating: 93 and 45 nm for PS(23)-*b*-PANa(160) and 110 and 55 nm for PS(86)-*b*-PANa(190). Thus, all the samples in the present study were heated for 5 days prior to molecular weight determination by SLS, to ensure a high extent of disentanglement.

The question of dynamics in the cores of the present micelle system deserves some consideration. Initially, micelle formation occurred when the block copolymers were dissolved in methanol during the neutralization of the poly(acrylic acid) (PAA) blocks. Since methanol is a nonsolvent for PS, the micelle cores would be expected to be solvent-free and glassy. Thus, the exchange between single chains and micelles would be expected to be very slow. The micelles were then freeze-dried and redissolved in water, and the solutions were heated at 100 °C. The glass transition temperatures (T_g) of the PS core for the molecular weight range investigated, i.e., between 6.2×10^2 and 9.0×10^3, were estimated[35] to be below 100 °C. The PS cores at that temperature are thus not glassy, and the kinetics in the system is expected to increase, resulting in the possible exchange of single chains with micelles. Thus, in addition to dissociating the entanglements in the PANa chains, heating the solutions may also increase the mobility in the micelle system, resulting in equilibrium micelle structures. At room temperature, most of these structures would be expected to be "frozen"; this aspect will be discussed in section 3.3.3.

3.3. Aggregation Numbers and Micellar Sizes as a Function of Salt Concentration. 3.3.1. Specific Refractive Index Increment. The specific refractive index increments (dn/dc) of some block polyelectrolytes were determined in water and in aqueous solutions of different NaCl concentrations. The values are given in Table 2. In deionized pure water, the dn/dc values were found to be independent of either the PS or the PANa block lengths for the range of block copolymers investigated, yielding the number 0.222 ± 0.003 mL/g. This value is similar to that given in the literature for poly(sodium acrylate), i.e., 0.231 mL/g, reported at a wave-

Table 2. Specific Refractive Index of Poly(styrene-*b*-sodium acrylate) in Water and in NaCl Solutions

PS(*X*)-*b*-PANa(*Y*)	d*n*/d*c* (mL/g)	solvent
23-*b*-44	0.227 ± 0.004	water
23-*b*-81	0.221 ± 0.002	water
50-*b*-300	0.220 ± 0.007	water
71-*b*-500	0.220 ± 0.004	water
average	**0.222** ± 0.003	**water**
23-*b*-300	0.201 ± 0.004	0.025 M
23-*b*-300	0.201 ± 0.003	0.050 M
23-*b*-300	0.170 ± 0.002	0.10 M
23-*b*-160	0.174 ± 0.004	0.10 M
average	**0.172** ± 0.002	**0.10 M**
23-*b*-300	0.173 ± 0.007	1.0 M
23-*b*-300	0.163 ± 0.005	2.5 M

length of 546 nm;[36] the value for the present study is expected to be lower, in view of the wavelength of light used (630 nm).

The change in the d*n*/d*c* values with block length has been found to be negligible for block copolymers which have a small weight fraction of one of the blocks.[30] This situation should be valid in the present case, since the micelles consist of a highly expanded polyelectrolyte corona and a small compact core. The core is also expected to be solvent-free, since the interactions between polystyrene and water are extremely unfavorable. A comparison of the R_g values, which would be lower than the hydrodynamic radii, with the calculated R_c values (eq 5), shows that the core is, indeed, very small (Table 1). The micellar core is thus expected to be much smaller than the corona, and the d*n*/d*c* should not be affected by the composition of the micelles.

Because the d*n*/d*c* values were found to be independent of the polymer composition, the apparent molecular weight can be assumed to be close to the true molecular weight. This fact has been observed for several micellar systems, either because of the similarity in the refractive indices of the two blocks[37] or because of the fact that the insoluble block consists of only a small fraction of the polymer and thus does not have a great effect on the d*n*/d*c* values.[38]

Since the change in the d*n*/d*c* values for different block lengths has been found to be negligible, the d*n*/d*c* values in different salt solutions were determined for only two block polyelectrolytes, PS(23)-*b*-PANa(300) and PS(23)-*b*-PANa(160). The d*n*/d*c* values of the dialyzed PS(23)-*b*-PANa(300) solutions were measured in different NaCl concentrations, ranging from 0.025 to 2.5 M. These results are also given in Table 2. For salt concentrations of 0.025 and 0.05 M, the d*n*/d*c* values remained constant at 0.201 mL/g. For 0.10 M, the d*n*/d*c* value was found to be 0.170 ± 0.002 mL/g. The d*n*/d*c* of PS(23)-*b*-PANa(160) measured in 0.10 M NaCl was 0.174 ± 0.004 mL/g, which was in agreement with the d*n*/d*c* value of PS(23)-*b*-PANa(300). For higher salt concentrations, i.e., 1.0 and 2.5 M, the d*n*/d*c* values were found to be 0.173 and 0.163 mL/g, respectively. A linear regression analysis was performed for the d*n*/d*c* values as a function of salt for the data at 0.10, 1.0, and 2.5 M NaCl. It was found that the intercept and slope of the line was 0.174 and −0.0040, respectively. Therefore, from the linear regression, the d*n*/d*c* values for salt concentrations ranging between 0.10 and 2.5 M, which were not directly measured, were calculated.

The d*n*/d*c* values of poly(sodium acrylate) determined at different wavelengths of measurement have been reported previously in the literature by different researchers.[36-41] They were found to depend both on the degree of neutralization[39] and on the salt concentration.[39-41] It was found that the values were essentially constant below 0.10 M, but above 0.10 M, they decreased gradually with increasing salt content, due to the increasing refractive index of the solvent medium.[40,41] However, in the present system, a different trend of d*n*/d*c* with salt concentration was observed. For low salt concentrations (<0.10 M), the d*n*/d*c* values decreased significantly but decreased only slightly for higher salt concentrations.

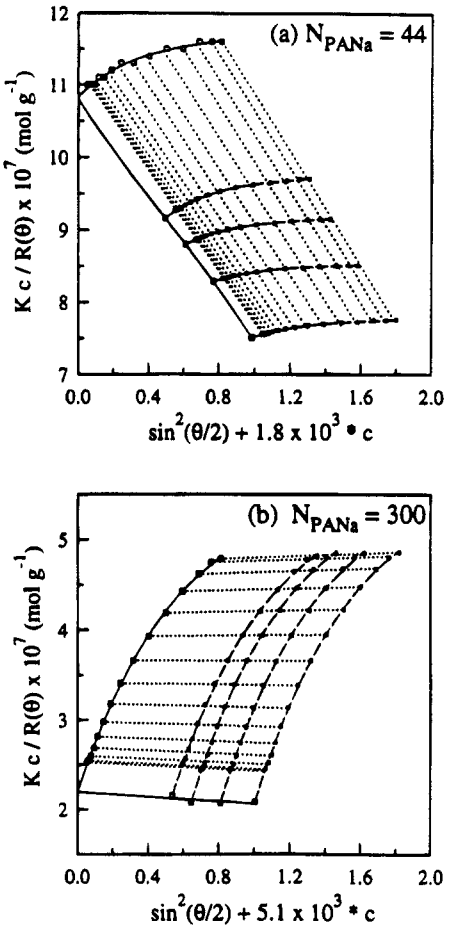

Figure 2. Typical Zimm plots for (a) PS(23)-*b*-PANa(44) and (b) PS(23)-*b*-PANa(300) in 2.5 M NaCl.

3.3.2. Typical Zimm Plots. Typical Zimm plots for polyelectrolyte micelles are given in Figure 2, plotted with a positive scaling factor, *k*. The graphs were chosen to illustrate a range of features typically found in such block copolymer micelles. The Zimm plots show the results for a constant PS block length of 23 units and different PANa block lengths of 44 (a) and 300 (b) units in 2.5 M NaCl. The effects of the PANa block length on the radius of gyration, aggregation number, and second virial coefficient values as obtained for these two systems are given in Table 1.

First, it is interesting to compare the angular dependence of the Zimm plots for PS(23)-*b*-PANa(44) and PS(23)-*b*-PANa(300). The angular dependence of the sample with the longer PANa block (Figure 2b) exhibits more curvature than that with the shorter PANa block (Figure 2a). Consequently, the dissymmetry ratios for the PANa block lengths of 300 and 44 units were 1.7 and 1.0, respectively. The micelles formed from block copolymer containing 300 PANa units have a larger radius of gyration (90 nm) than that of the micelles with

Table 3. Micellar Properties of Some Poly(styrene-*b*-sodium acrylate) Block Polyelectrolytes Micelles in Different Salt Concentrations[a]

PS(X)-*b*-PANa(Y)	C_s (M)	$M_w \times 10^{-6}$	N	$R_g^{(a)}$ (nm)	$R_g^{(b)}$ (nm)	$A_2 \times 10^4$ (mL mol/g^2)	Z_d
6-*b*-180	0.025	0.19	12	87	75	3.25	2.1
	0.050	0.19	11	50	42	0.92	1.3
	0.10	0.43	24	46	34	0.87	1.2
	1.5	0.41	24	48	32	0.028	1.2
	2.5	0.45	26	37	30	−0.20	1.2
23-*b*-300	0.050	2.7	87	90	80	2.13	1.7
	0.10	3.8	120	96	85	0.45	1.7
	0.25	4.6	150	93	82	−0.21	1.7
	0.50	4.4	150	93	82	−0.42	1.7
	1.0	4.6	150	95	85	−0.13	1.7
	1.5	4.6	150	95	85	−0.17	1.7
	2.5	4.5	150	90	80	−0.36	1.7

[a] The R_g values were evaluated in (a) from either a Debye or a Zimm plot and in (b) from linear extrapolations of Debye plots excluding higher angles. The calculations for N were done using three significant figures and subsequently rounded to two significant figures.

44 PANa units (30 nm). This result is expected, since the size of the micelles is related to the dimensions of the block copolymer. The aggregation numbers of these two samples in 2.5 M salt are similar in magnitude, 140 and 150 for PS(23)-*b*-PANa(44) and PS(23)-*b*-PANa(300), respectively.

The second virial coefficient was evaluated from the concentration dependence of the light scattering data extrapolated to an angle of 0°. For the sample with the longer PANa block (300), the second virial coefficient in 2.5 M salt solution is greater than that of the sample with a shorter PANa block (44). The A_2 values for the 300 and 44 PANa unit lengths were -0.36×10^{-4} and -3.5×10^{-4} mL mol/g^2, respectively. These values suggest that the sample with the longer PANa chains is in a more favorable solvent than that with shorter PANa chains, perhaps because the longer PANa units solvate the micelle to a greater extent. As the soluble block length increases, it is expected that the solubility of the block copolymer will also increase. This result can be understood by considering that an increase in the PANa length results in an increase in the corona density and hence a reduction in the unfavorable interactions between the hydrophobic core and the solvent. A similar trend in A_2 has been reported previously for PS-*b*-PEO in cyclopentane.[10]

All the samples listed in Table 1 exhibited a linear dependence of $Kc/R(\theta)$ on the concentration. This result indicates that these micelles remain stable in the concentration range studied. Furthermore, the solutions can be seen to be in a dilute state, since the effects of the higher virial coefficients are negligible. In many block polyelectrolyte samples, the angular dependence of the $Kc/R(\theta)$ was nonlinear, which is expected for large particles. As mentioned previously in section 3.1, for large particles, the Debye plot gives a better estimate of M_w and R_g. In the present system, it was found that, for Z_d values below 1.7, the Debye and Zimm plots gave the same results. However, for particles which had Z_d values equal to and above 1.7, the Debye plot was used for a more accurate evaluation. In the present system, the R_g values were also determined from linear extrapolations of the $\theta = 0°$ line from the Debye plots, in which the values at high angles, where the points deviate significantly from linearity, were omitted. These results are summarized in Tables 1 and 3 and will be discussed in the subsequent sections.

3.3.3. Influence of Salt Concentration. The influence of a broad range of NaCl salt concentrations (C_s) on the micellar properties was explored for two block polyelectrolyte samples, PS(6)-*b*-PANa(180) and PS(23)-*b*-PANa(300). The results for the weight-average molecular weight (M_w), aggregation number (N), radius of gyration values (R_g), second virial coefficient (A_2), and dissymmetry ratio are given in Table 3. The aggregation numbers can be described by two regions, depending on the magnitude of C_s. For low salt concentrations, the aggregation numbers were found to increase with increasing salt concentration. For instance, the N values for PS(6)-*b*-PANa(160) in 0.050 and 2.5 M NaCl increased from 11 to 26, respectively. Similarly, for PS(23)-*b*-PANa(300), the N values in 0.050 and 2.5 M NaCl increased from 90 to 150, respectively. At higher salt concentrations (>ca. 0.10 M), the aggregation numbers were found to remain essentially constant. This result can also be seen in Table 1, which shows that the N values for PS(6)-*b*-PANa(89) and PS(6)-*b*-PANa(400) were essentially the same in 0.10 and 2.5 M NaCl. Similar results for the dependence of N on salt concentration have been obtained by Selb and Gallot in a mixed solvent system of water−methanol−LiBr.[1] For a typical polymer, e.g., PS(26)-*b*-P4VPEtBr-(140), N increased at low salt concentrations and remained essentially constant above 0.2 M LiBr. It should be noted that, for a very low salt concentration (0.01 M), no micelles were seen for that sample.

It is interesting to note that micelles based on the block copolymer samples discussed above, i.e., PS(6)-*b*-PANa(180) and PS(23)-*b*-PANa(300), appear to have a structure which is not frozen, since N is a function of the salt concentration. In general, it has been found that if the solvent is extremely unfavorable for the block forming the core, the micelle structure can be frozen,[42] especially if the T_g of the core is above room temperature. In the present case, the fact that N changes with salt concentration might be due to the concentrations used in the study of these two samples, which were only ca. 2−6 times higher than the cmc values as determined previously.[9] Therefore, the system might still be in equilibrium since the concentrations are in the vicinity of the cmc. It would be expected that for longer PS block lengths, N would be unaffected by the salt concentration since the micelles might already be frozen. It should also be borne in mind that for a PS block size of 6 units, the glass transition temperature is estimated to be ca. 260 K,[35] i.e., below room temperature, which would contribute to the fluidity of the micelles.

The behavior of the aggregation numbers as a function of salt content can be explained by considering the behavior of block polyelectrolyte micelles in different salt concentrations. According the theory of Marko and Rabin,[22] micelle formation in block polyelectrolytes is determined by a balance of the core−solvent interface energy and Coulombic repulsions of the charged polyelectrolyte chains. In block polyelectrolyte micelles, electrostatic effects play a major role in micelle formation and predominate at low salt concentrations. According to this theory, micelle formation will not occur for highly charged diblock polyelectrolytes because of the strong electrostatic repulsive forces along the chain. At low salt concentrations, as described by Dan and Tirrell,[23] electrostatic correlations dominate the chain configurations, and thus also the aggregation behavior. As the salt concentration increases from very low concentrations, the electrostatic repulsions decrease and

the aggregation number increases. At moderate salt concentrations, the aggregation numbers do not vary significantly with the addition of salt and the micellar properties are dominated by the core block properties. Therefore, N, the cmc, and the chemical potential of the micelles are identical to those calculated for micelles of neutral diblock copolymers. However, the size of the corona is a function of the salt concentration.

Polyelectrolyte chains in water or in low salt concentrations expand due to electrostatic repulsions of the charges on the polymer backbone. This phenomenon is known as the polyelectrolyte effect. For the samples investigated, this effect was observed for only one sample, PS(6)-*b*-PANa(180) in 0.025 M NaCl. The R_g for this sample in 0.025 M NaCl is ca. 2 times larger than the value at higher salt concentrations. Table 3 shows the R_g values as a function of salt concentration; it is observed that, with that one exception, the R_g values do not vary significantly with the C_s. However, it should be noted that since SLS is more sensitive to larger particles in solution, the effects of salt on the single chains cannot be observed. It is conceivable that the dimensions of these chains are affected by the salt content to a greater extent than those of the micelles.

The dimension of the micelle with the polyelectrolyte chains in a fully extended conformation can be evaluated simply and is done here for the PS(6)-*b*-PANa(180) block polyelectrolyte. For instance, assuming a bond length of 0.25 nm per repeat unit and using the calculated value for the radius of the core, 2 nm (Table 1), the radius of the micelle with fully extended polyelectrolyte arms is ca. 50 nm. A comparison of this value with the R_g values determined experimentally by the Debye plot using all angles in a nonlinear extrapolation ($R_g^{(a)}$) or using only the low angles in a linear extrapolation ($R_g^{(b)}$), 87 or 75 nm, respectively, suggests that the polyelectrolyte chain must be in a highly extended conformation. The experimental R_g values are larger than the calculated value. This difference is possibly due to the polydispersity of micelle sizes,[43] since the calculated value is based on a number-average value, while the R_g values obtained from SLS measurements are z-average values.

The quality of the solvent for the block polyelectrolyte micelles as a function of salt concentration was evaluated from the second virial coefficient values. The A_2 values for the present system are given in Table 3. These values were found to decrease with increasing salt concentration. This result is consistent with the trend observed for polyelectrolyte solutions.[44] The A_2 values were also found to have a linear dependence on the inverse salt concentration (C_s^{-1}). This relation is illustrated in Figure 3 on a semilog plot; in the inset, the C_s^{-1} axis is given as a linear scale. It should be noted that the A_2 values agree with those previously reported for poly(sodium acrylate), with molecular weights ranging from 3×10^4 to 6.4×10^5.[45] These values are represented in Figure 3 as filled squares. Thus, within experimental error, the A_2 values do not differ significantly for the samples investigated in which the M_w of the PANa block ranged from 1.7×10^4 to 2.8×10^4.

The Θ point for these samples was evaluated to be at ca. 0.3 M NaCl, from Figure 3. It should be mentioned that, at salt concentrations above 2.5 M, the A_2 values appeared to increase, i.e., become positive. This phenomenon has been observed in other systems, such as cationic polyelectrolytes[46] and polystyrene latexes stabilized by a graft copolymer of PAA.[47] However, since

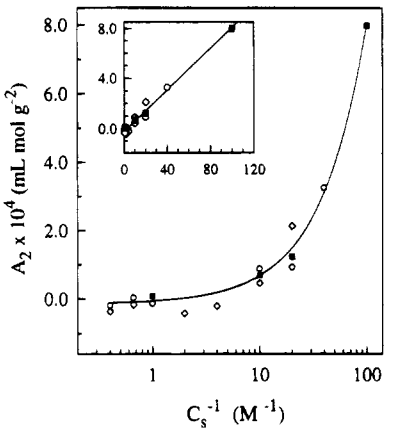

Figure 3. Second virial coefficient values for samples PS(6)-*b*-PANa(180) (○), PS(23)-*b*-PANa(300) (◇) and poly(sodium acrylate) (■)[45] as a function of the inverse salt concentration on a semilog plot. The inset graph shows the relation on a linear plot.

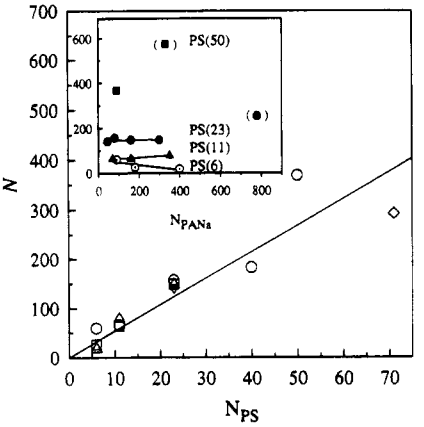

Figure 4. Aggregation number as a function of insoluble PS block length for almost constant PANa block lengths of 85 (○), 170 (□), and 350 (Δ) units as well as the samples PS(23)-*b*-PANa(44) (▽) and PS(71)-*b*-PANa(120) (◇). The inset graph shows the aggregation number as a function of PANa block length for constant PS block lengths, and the points in parentheses represent the samples PS(50)-*b*-PANa(330) and PS(23)-*b*-PANa(780).

the dn/dc values were not determined for salt concentrations above 2.5 M, the magnitude of A_2 values for higher salt concentrations cannot be quantified. The decrease in the solvent quality as a function of salt concentration for these block polyelectrolyte micelles will be addressed in a subsequent paper dealing with the phase separation of these micelles at very low concentrations.[48]

3.4. Characterization in 2.5 M NaCl. 3.4.1. Aggregation Numbers and Calculated Core Radii. The results obtained from static light scattering for the weight-average molecular weights, aggregation numbers, and radii of gyration for the samples investigated are summarized in Table 1. The aggregation numbers and radii of gyration will also be discussed in some detail in the section dealing with the application of various micelle theories (section 3.5). However, it is interesting at first to examine the effect of the soluble and insoluble block length on the aggregation numbers.

The inset of Figure 4 shows the aggregation numbers plotted as a function of the PANa block length for various PS block lengths. For the series consisting of PS block lengths of 6, 11, and 23 units, the N values were found to show a slight dependence on the PANa block length. For the series consisting of a PS block

length of 6 units, the aggregation numbers decreased as the soluble block length increased. For instance, as the PANa block length increased from 89 to 180 to 400 units, the aggregation numbers decreased from 59 to 26 to 18, respectively. This result agreed with previously reported results for different micellar systems, PS-*b*-P4VPEtBr[1] and PS-*b*-PEO,[49] for which it was observed that as the length of the soluble block increased, the aggregation number decreased.

For the PS(11) and PS(23) series, N increased only slightly with increasing PANa block length. The mean N values and their standard deviations for the PS(11) and PS(23) series (excluding the sample with the longest PANa block length, PS(23)-*b*-PANa(780)) were 69 ± 9 and 148 ± 6, respectively. It has been previously reported by Selb and Gallot that once the block forming the micelle core exceeds a certain length, micellization is predominately determined by the core block properties and not those of the soluble block.[1] This result was also seen in the previous paper in this series, where it was observed that the effect of the PANa block length on the cmc decreased with increasing PS block length.[9] For the PS(50) series, it was found that N increased considerably with increasing PANa block length. However, it should be noted that the PS(23)-*b*-PANa(780) and PS(50)-*b*-PANa(330) samples showed a much higher N than the other samples in the series (shown in parentheses in the inset of Figure 4). These two samples also deviated from theoretical scaling predictions for N and R_c, as will be seen in section 3.5. Therefore, if the two samples [PS(23)-*b*-PANa(780) and PS(50)-*b*-PANa(330)] are omitted, there is not a significant dependence of the soluble block length on N.

It is of interest to examine the dependence of the aggregation numbers on the insoluble block length. The plot of N as a function of PS block length, for all the points given in Table 1, is shown in the main part of Figure 4. The only samples omitted were PS(23)-*b*-PANa(780) and PS(50)-*b*-PANa(330), for reasons discussed previously. For convenience, the symbols represent samples with different PS block lengths but approximately constant PANa block lengths selected from Table 1. The three different PANa block lengths were 85 ± 4 (○), 170 ± 7 (□), and 350 ± 30 (△) PANa units. For completeness, the results for samples PS(23)-*b*-PANa(44) and PS(71)-*b*-PANa(120), which had PANa block lengths different from those three block lengths, were also plotted. It was found that a common line could be drawn through all the points, regardless of the PANa block length. This fact confirms that there is not a significant dependence on the PANa block length on N, as was discussed previously. From the slope of the line fitted through zero, the change in N with PS block length was evaluated. For instance, when the PS block was varied from 10 and 50 units, the aggregation numbers increased from 54 to 270. Thus, it is seen again that the effect of the insoluble block length on N is thus much greater than that of the soluble block length.

The values of the surface area per chain (S/N), evaluated from eq 6, are given in Table 1. These values were found to increase with increasing PS block length. A linear plot of the S/N values as a function of the PS block length (graph not shown) was found to have the linear regression

$$S/N = 1.47 + 0.027N_{PS} \quad (8)$$

with a correlation coefficient of 0.87. It is interesting to note that the slope of this line is similar in magnitude to that obtained for micelles of PS-*b*-PAA in water (0.025).[50] These latter samples resemble crew-cut micelles[51] since they are composed of long PS block, ca. 170−1400 units and relatively short PAA blocks. The S/N values were also compared to those of the reverse micelle system, poly(styrene-*b*-cesium acrylate),[12] (PS-*b*-PACs), poly(styrene-*b*-cesium methacrylate) (PS-*b*-PMACs)[12] and poly(styrene-*b*-4-vinylpyridinium methyl iodide) (PS-*b*-P4VPMeI)[52] in toluene. It was found that, for comparable core sizes, the dependence of S/N on the insoluble block for the reverse micelle systems was larger than that found in the present system. For the samples with micelle cores composed of PACs and PMACs, the slope from a plot of S/N as a function of core block length was 0.047 nm^2/chain, and for those composed of P4VPMeI the slope was 0.12 nm^2/chain. It should be mentioned that a second-order fit improved the regression coefficient for these two reverse micelle systems. Thus, the surface density of chains is larger in the present system, compared to that of the reverse micelle system. The differences in the S/N values might be due to the preparation conditions of the micelles, i.e., whether micellization occurs under equilibrium or nonequilibrium conditions. The importance of sample preparation for reverse micelles was examined by Nguyen et al.,[43] who investigated the core radii, aggregation numbers, and S/N values as a function of the ionic chain polydispersity index and method of preparation.

3.4.2. Second Virial Coefficient Values. The second virial coefficient values for associating systems, such as block copolymers, can be quite complex to analyze. This fact is due to the dependence of A_2 on several parameters, such as the interaction of both blocks with the solvent, the molecular weight, and the configuration or size of the molecules in solution. Since the block copolymers form micellar structures, it is sometimes difficult to separate the dependence of the A_2 values on the different parameters. Some workers[5] have found good agreement between experimental A_2 values and those calculated by using the hard-sphere model.[53] However, in the present case, this model was not found to describe the system.

The interpretation of the A_2 values in the present system is further complicated by the polyelectrolyte nature of the micelle corona. Many theories have been published which deal with the A_2 values for polyelectrolytes.[44] In some theories, polyelectrolytes were described as ideal spherical colloidal electrolyte particles. In this approximation, the A_2 values are proportional to the square of the number of charges and inversely proportional to the square of the molecular weight and salt concentration. These theories were then modified to account for two factors, the electrostatic interaction among the ions and the polymeric nature of the polyelectrolyte. The first term depends on the charge density of the polyelectrolyte, while the latter term is a function of the expansion factor. Due to the complexity of the present system, no trend for the A_2 values was observed. However, it was found that the block polyelectrolyte samples with the highest fraction of PS, such as PS(23)-*b*-PANa(44), had the lowest A_2 values. In general, as the fraction of PS decreased, the A_2 values increased. This result should be expected, as discussed in section 3.3.2., since the contribution of the unfavorable interactions between the PS core and aqueous solution would be minimized.

3.4.3. Radius of Gyration Values. As mentioned previously in section 3.3.2., for the present system the R_g values were evaluated by using all the data points either in a nonlinear expansion for $P(\theta)$ in a Zimm or a Debye plot ($R_g^{(a)}$) or from the slope of a linear extrapolation of a Debye plot, omitting the points at higher angles which deviate from linearity ($R_g^{(b)}$). The R_g values determined by these two methods are given in Table 1 for the samples in 0.1 and 2.5 M NaCl and in Table 3 for the samples in different NaCl concentrations. In general, the $R_g^{(b)}$ values were found to be smaller than the $R_g^{(a)}$ values. Also, it should be noted that the radii of gyration of some samples were found to be larger than the calculated radius of a micelle having a fully stretched corona block. In particular, this result was found for PS(6)-*b*-PANa(89), PS(11)-*b*-PANa(69), and block polyelectrolyte samples which were symmetric in the PS and PANa block lengths. This result may be due to polydispersity effects of the micelles, as discussed in section 3.3.3. Also, it has been found by Cogan et al.[54] that, for small symmetric copolymers of PS-*b*-PEO in cyclohexane with traces of water in the core, the coronal chains were found to be severely stretched in the intermediate region as compared to the behavior of asymmetric copolymers. This result is consistent with the present observations for the micelles formed from symmetric copolymers, which were found to be in a more stretched configuration relative to those formed from asymmetric copolymers.

3.5. Applications of Scaling Theories. Since data have been obtained for a wide range of block polyelectrolytes in aqueous solutions, it was of interest to interpret the results for the present block polyelectrolytes according to the various models which are available. In this section, scaling theories for the star model and the mean-field models will be applied to the PS-*b*-PANa system in 2.5 M NaCl. It should be recalled that the block copolymers may have been in a mobile state when heated at 100 °C. However, at room temperature most of these micelles are in a frozen state, especially those with very long PS block lengths.

3.5.1. Star Model. One scaling model which is relevant is that of Dan and Tirrell,[23] which suggests that, at intermediate salt concentrations, the micellar parameters scale according to Halperin's star model.[20] In this section, the scaling relations of the star model for N, calculated R_c, and R_g will be investigated for block polyelectrolyte micelles in 2.5 M NaCl according to the scaling relations of the star model.

The model predicts that the aggregation number of the micelles is proportional to $aN_B^{4/5}$, where a is the monomer size and N_B is the length of the insoluble block. This scaling relation was found to give a satisfactory description of the micelles in 2.5 M NaCl (graph not shown). The linear regression was $N = -5.9 + 12\ N_B^{4/5}$, with a correlation coefficient of 0.86. This result shows that the aggregation numbers of the block polyelectrolyte micelles are independent of the ionic block length within the confidence intervals of the linear regression. However, it should be recalled that some effects of the soluble block on N or R_c were observed (Figure 4). The intercept of the line (−5.9) can also be taken as being essentially zero, since typical values of N range from 20 to 400. It should be noted that the block copolymers of composition PS(50)-*b*-PANa(330) and PS(23)-*b*-PANa(780) were omitted from the analysis of the linear regression. These two block copolymers form micelles which have the highest molecular weight of all the samples investigated and do not fit the scaling relation. It might be possible that the scaling relations fail for these high aggregation numbers or that since these samples contain the longest soluble block for the two series, they might contain some supermicellar structures.

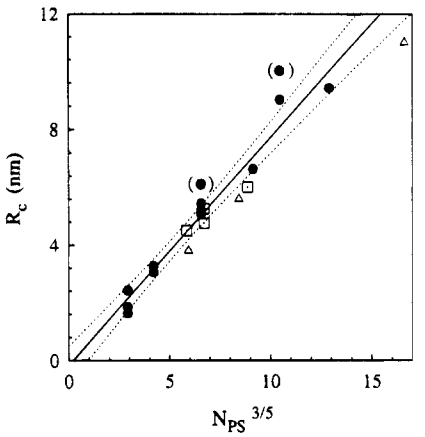

Figure 5. Radius of the core as a function of the PS block length to the power of $^3/_5$, according to the star model for PS-*b*-PANa in 2.5 M NaCl (●), PS-*b*-PMACs and PS-*b*-P4VPMeI in the solid state (⊡),[55] and PS-*b*-PEO in water (△).[49] The solid line represents the linear regression through the data, and the dashed line represents the 95% confidence limits.

The Halperin star model also suggests that the scaling relation between the core radius and the length of the insoluble block is $R_c \propto aN_B^{3/5}$. Figure 5 shows the calculated core radii plotted according to the above relation for the block polyelectrolyte micelles (filled circles). The solid line represents the linear regression through the points, and the dotted line represents the 95% confidence limit intervals, excluding the two block copolymer samples PS(50)-*b*-PANa(330) and PS(23)-*b*-PANa(780) (shown in parentheses), as was previously mentioned. The slope of the line is 0.79 nm/(PS repeat unit)$^{3/5}$, with an intercept of essentially zero (−0.16) and a correlation coefficient of 0.98. This result shows that, within the 95% confidence interval, R_c is independent of the ionic block length, as was also seen in the scaling behavior for aggregation numbers.

The same scaling behavior for R_c has also been found to apply to reverse micelles as investigated recently by small-angle X-ray scattering (SAXS),[12,52] which allows the measurement of the core radius directly. The reverse micellar systems investigated consisted of a soluble polystyrene corona attached to an insoluble ionic block composed of either PACs,[12] PMACs,[12] or P4VPMeI in toluene.[52] The mirror system, forming regular micelles consisting of a PS core and a PACs corona, was also studied in the solid state by SAXS.[55] The prefactors, which are proportional to the typical monomer size, a, for the reverse and regular micelles, were found to be 0.91 and 0.72 nm/(repeat unit)$^{3/5}$, respectively, which seemed reasonable in view of the differences in the monomer volumes.[55]

According to the star model, the radius of the micelle is proportional to $N_B^{4/25}N_A^{3/5}$. This scaling relation was investigated using the two series of R_g values evaluated (Table 1). The linear relation for both R_g values as plotted according to the star model for the 2.5 M salt solution had a correlation coefficient of 0.69. The relation using $R_g^{(a)}$ was found to have a higher slope; however, the line was within the confidence limit intervals of that using $R_g^{(b)}$. Figure 6 shows the relationship of $R_g^{(b)}$ to the block lengths according to the

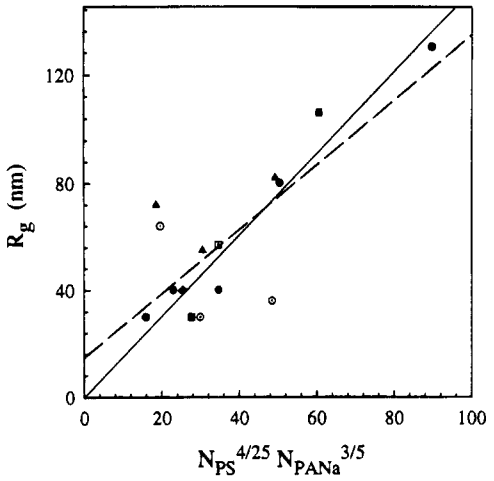

Figure 6. Radius of gyration ($R_g^{(b)}$) according to the scaling predictions of the star model for PS-*b*-PANa in 2.5 M NaCl for different PS block lengths of 6 (⊙), 11 (▲), 23 (●), 40 (◆), 50 (■), and 71 (⊡) units. The points in parentheses represent the samples PS(50)-*b*-PANa(330) and PS(23)-*b*-PANa(780). The lines represent linear regressions through the data; the dashed line is the best fit, and the solid line is forced through the origin.

above scaling relation; the dotted line represents the linear regression through the data, and the solid line represents a linear regression which was forced through the origin.

3.5.2. Mean Field Models. In addition to the star model, there are mean-field theories which give scaling relations for several micellar parameters. In general, these theories describe micelles formed from relatively large cores and small coronas. These models therefore do not describe star-type micelles; however, it was still of interest to apply these models to the present system. In this section, the results of the SLS measurements will be compared with four mean-field theories, those of de Gennes,[13] Leibler et al.,[15] Whitmore and Noolandi,[16] and Nagarajan and Ganesh.[18]

The theories by de Gennes[13] and Leibler et al.[15] describe the micelle properties as being dominated by the insoluble block. The scaling relations given by de Gennes are $R_c \propto N_B^{2/3}$ and $N \propto N_B$. Similarly, the scaling relations obtained by Leibler et al. were $R_c \propto N_B^{0.53}$ and $N \propto N_B^{0.6}$. The correlation coefficients for the line using these scaling relations are given in Table 4. It can be seen that good agreement is obtained.

The theories by Whitmore and Noolandi[16] and by Nagarajan and Ganesh[18] suggest scaling relations for the micellar parameters which are proportional to $N_A^{\alpha} N_B^{\beta}$. In the theory by Whitmore and Noolandi, the structural parameters were determined for block copolymers in a homopolymer of A.[16] The exponents of the scaling relation for the R_c values were found to fall within a range; for example, for α the range was from -0.1 to 0 and for β it was from 0.67 to 0.76.

The α exponent for the present system was determined by plotting the log of the micellar parameter as a function of log N_A for a constant N_B. Similarly, for the evaluation of β, the log of the micellar parameters were plotted as a function of log N_B for a constant N_A. It should be mentioned that the two samples having the highest aggregation numbers are omitted for the present discussion. The values of the β exponents for R_c and N were found to be 0.67 and 1, respectively. It is interesting to note that these exponents are the same as those proposed by de Gennes.[13] The evaluation of the α exponent was not quite as clear, since, as shown in Figure 4, the dependence of N on the soluble block length varied as a function of the PS block in some cases. The values of α for R_c and N were found to be (-0.3, 0.05, and 0.006) and (-0.8, 0.2, and 0.01), respectively, for PS block lengths of 6, 11, and 23 units. In view of the large standard deviation for these values, the exponents were taken as being essentially zero. The correlation coefficients for the lines $R_c \propto N_B^{0.67} N_A^0$ and $N \propto N_B N_A^0$ were 0.97 and 0.83, respectively, and were thus found to agree with the relations of de Gennes. The scaling relations according to these two theories are summarized in Table 4. It was found that the mean-field theories mentioned above are applicable to the present system.

3.6. Comparison with Solid-State Results and with Those for PS-*b*-PEO in Water. In Figure 5, the core radii for the 2.5 M salt concentration were compared with the values obtained from the solid state, represented as dotted squares. The solid-state results were determined in an independent study of block polyelectrolytes by SAXS.[55] In that study, the core radii were measured for three PS-*b*-PMACs and one PS-*b*-P4VPMeI samples which were cast from tetrahydrofuran–methanol (70:30, v/v) or DMF–water (95:5, v/v) mixtures, respectively. The solvent was evaporated slowly, and the films were subsequently dried. The resulting morphology consists of a collapsed PS block surrounded by either a soluble PMACs or P4VPMeI block. In the solid state, the styrene core is embedded in a continuum of PMACs. The agreement of the R_c values for the samples in solution and those in the solid state was within the 95% confidence limits. Agreements between solid and solution results have been observed previously, for example, in block ionomer reverse micelles.[52] Agreement would be expected, since the micelle morphology is expected to be retained during solvent evaporation, once micelle formation has occurred.[56]

Two conclusions can be made based on the agreement of the core radii in the 2.5 M salt solution and in the solid state. First, for the 2.5 M salt concentration, the core radii were determined from calculations based on the aggregation numbers. Therefore, it can be assumed that, in the 2.5 M salt concentration, the polyelectrolyte corona does not form supermicellar structures. Clearly, if some supermicellar structures were present in the solution, then the calculated R_c values would be significantly larger than those obtained from the solid state. Second, the agreement also shows that the core in the 2.5 M salt concentration is solvent-free, since the two values agree. This result is expected because of the extremely unfavorable interaction between PS and water.

It is also of interest to compare the results of the present system with those of a nonionic hydrophilic system, PS-*b*-PEO in water.[49] In that study, it was found that two populations of particles are present in solution, regular micelles and loose micellar clusters consisting of tens of micelles. The presence of clusters is not surprising since it has been observed by SLS that poly(ethylene oxide) forms intermolecular associations due to hydrophobic interactions.[57] Also, a recent study investigated the formation of these PEO clusters, which coexist with molecularly dissolved PEO, by a variety of techniques, including DLS, SLS, and size-exclusion chromatography (SEC).[58] The R_c values for the regular micelles formed from three samples, PS(108)-*b*-PEO(400), PS(35)-*b*-PEO(450), and PEO(102)-*b*-PS(39)-*b*-PEO-

Table 4. Summary of Results Obtained for Different Theoretical Scaling Relations

theory	R_c	r^2 [a]	N	r^2 [a]	R_g	r^2
star model[19,20]	$N_B^{3/5}$	0.98	$N_B^{4/5}$	0.86	$N_A^{3/5}N_B^{4/25}$	0.69
de Gennes[13]	$N_B^{2/3}$	0.97	N_B	0.83		
Leibler[15]	$N_B^{0.53}$	0.98	$N_B^{0.6}$	0.87		
Whitmore–Noolandi[16] or Nagaragan–Ganesh[18]	$N_B^{0.67}N_A^0$	0.97	$N_BN_A^0$	0.83		

[a] Correlation coefficient evaluated omitting samples PS(23)-*b*-PANa(780) and PS(50)-*b*-PANa(330) (see text).

(102), were calculated from the aggregation numbers (eq 5).[49] These values are represented in Figure 5 as hollow triangles; for the triblock sample, half of the PS block length was used in the calculation for the plot. A comparison of these two systems illustrates the effect on the micellization behavior of block copolymers having an insoluble PS block attached to either an ionic or a nonionic soluble block. It can be seen that the values for the core radii of the PS-*b*-PEO in water are very similar in magnitude to those of the present block polyelectrolyte system. This result is to be expected, since the nature of the core is the dominant factor in micellization.

4. Conclusions

The block polyelectrolyte micellar system of poly(styrene-*b*-sodium acrylate) was investigated in aqueous media. First, it was found that heating the solutions for 5 days at 100 °C resulted in the dissociation of supermicellar aggregates, which are encountered upon sample dissolution. These supermicellar structures were postulated to exist as a result of the ionic interactions in the block polyelectrolytes in the phase-separated solid-state morphology. As was observed by studying the disentanglement process for different block polyelectrolytes, the samples which had shorter PANa lengths dissociated faster. To a first approximation, this process was found to be independent of the PS block length.

Two block polyelectrolyte samples were investigated as a function of NaCl concentration. It was found that at low salt concentrations, the aggregation numbers initially increased with increasing salt concentration and then eventually leveled off. The R_g values were independent of C_s, except for PS(6)-*b*-PANa(180) in 0.025 M NaCl. The second virial coefficient values decreased linearly with the inverse salt concentration, and the values agreed with literature values for PANa.[45]

For the block polyelectrolyte system in 2.5 M NaCl, good agreement was obtained between the micellar parameters and the scaling relations of the star and some mean-field models. In general, it was found that for the present system the aggregation numbers and the calculated core radii were essentially independent of the length of the soluble block within the confidence intervals of the linear regression. The calculated core radii values for samples in 2.5 M NaCl were found to be in good agreement with those determined previously in the solid state by SAXS. The R_c values were also found to be similar to those of PS-*b*-PEO in water.

Acknowledgment. We thank Dr. Xing Fu Zhong, who synthesized the block copolymers in connection with another project. We also thank Dr. Raymond J. Barlow for useful discussions and Dr. Joon S. Kim and Mr. Matthew Moffitt for helpful suggestions. This work was supported by the Natural Science and Engineering Research Council of Canada (NSERC). K.K. also thanks FCAR (Le Fonds pour La Formation de Chercheurs et L'Aide à la Recherche) and NSERC for scholarship funding.

References and Notes

(1) Selb, J.; Gallot, Y. In *Polymeric Amines and Ammonium Salts;* Goethals, E. J., Ed.; Pergamon Press: New York, 1980; pp 205–218.
(2) Price, C. In *Development in Block Copolymers;* Goodman, I., Ed.; Elsevier Applied Science: London, 1982; Vol. 1, pp 39–80.
(3) Riess, G.; Hurtrez, G.; Bahadur, P. *Encyclopedia of Polymer Science and Engineering;* Kroschwitz, J., Mark, H. F., Bikales, N. M., Overberger, C. G., Menges, G., Eds.; Wiley: New York, 1985; Vol. 2, pp 324–434.
(4) Selb, J.; Gallot, Y. In *Development in Block Copolymers;* Goodman, I., Ed.; Elsevier Applied Science: London, 1985; Vol. 2, pp 27–96.
(5) Tuzar, Z.; Kratochvíl, P. In *Surface and Colloid Science;* Matijevic, E., Ed.; Plenum Press: New York, 1993; Vol. 1, pp 1–83.
(6) (a) Rolland, A.; O'Mullane, J.; Goddard, J.; Brookman, L.; Petrak, K. *J. Appl. Polym. Sci.* **1992**, *44*, 1195. (b) El-Nokaly, M. A., Piatt, D. M., Charpentier, B. A., Eds. *Polymeric Delivery Systems: Properties and Applications;* ACS Symposium Series 520; American Chemical Society: Washington, DC, 1993. (c) Kwon, G.; Suwa, S.; Yokoyama, M.; Okano, T.; Sakurai, Y.; Kataoka, K. *J. Controlled Release* **1994**, *29*, 17.
(7) (a) Fendler, J. H.; Fendler, E. J. *Catalysis in Micellar and Macromolecular Systems;* Academic Press: New York, 1975. (b) Kitahara, A. *Adv. Colloid Interface Sci.* **1980**, *12*, 109.
(8) Astafieva, I., Zhong, X. F., Eisenberg, A. *Macromolecules* **1993**, *26*, 7339.
(9) Astafieva, I., Khougaz, K.; Eisenberg, A. *Macromolecules* **1995**, *28*, 7127.
(10) Vagberg, L. J. M.; Cogan, K. A.; Gast, A. P. *Macromolecules* **1991**, *24*, 1670.
(11) Xu, R.; Winnik, M.; Riess, G.; Chu, B.; Croucher, M. D. *Macromolecules* **1992**, *25*, 644.
(12) Nguyen, D.; Williams, C. E.; Eisenberg, A. *Macromolecules* **1994**, *27*, 5090.
(13) de Gennes, P.-G. *Solid State Physics;* Liebert, J., Ed.; Academic Press: New York, 1977; Suppl. 14, pp 1–18.
(14) Noolandi, J.; Hong, M. H. *Macromolecules* **1983**, *16*, 1443.
(15) Leibler, L.; Orland, H.; Wheeler, J. C. *J. Chem. Phys.* **1983**, *79*, 3550.
(16) Whitmore, M. D.; Noolandi, J. *Macromolecules* **1985**, *18*, 657.
(17) Munch, M. R.; Gast, A. P. *Macromolecules* **1988**, *21*, 1360.
(18) Nagarajan, R.; Ganesh, K. *J. Chem. Phys.* **1989**, *90*, 5843.
(19) Zhulina, E. B.; Birshtein, T. M. *Vysokomol. Soedin.* **1985**, *27*, 511.
(20) Halperin, A. *Macromolecules* **1987**, *20*, 2943.
(21) Daoud, M.; Cotton, J. P. *J. Phys.* **1982**, *43*, 531.
(22) Marko, J. F.; Rabin, Y. *Macromolecules* **1992**, *25*, 1503.
(23) Dan, N.; Tirrell, M. *Macromolecules* **1993**, *26*, 4310.
(24) Marques, C.; Joanny, J. F.; Leibler, L. *Macromolecules*, **1988**, *21*, 1051.
(25) (a) Miklavic, S. J.; Marcelja, S. *J. Phys. Chem.* **1988**, *92*, 6718. (b) Mirsa, S.; Varanasi, S.; Varanasi, P. P. *Macromolecules* **1989**, *22*, 5173. (c) Pincus, P. *Macromolecules* **1991**, *24*, 2912. (d) Ross, R. S.; Pincus, P. *Macromolecules* **1992**, *25*, 2177. (e) Wittmer, J.; Joanny, J. F. *Macromolecules* **1993**, *26*, 2691. (f) Zhulina, E. B. *Macromolecules* **1993**, *26*, 6273. (g) Seidel, C. *Macromolecules* **1994**, *27*, 7085. (h) Misra, S.; Mattice, W. L.; Napper, D. H. *Macromolecules* **1994**, *27*, 7090.
(26) (a) Ronis, D. *Macromolecules* **1993**, *26*, 2016. (b) Ronis, D. *Phys. Rev. E* **1994**, *49*, 5438.
(27) Huglin, M. B. Ed. *Light Scattering from Polymer Solutions;* Academic Press: New York, 1972.
(28) Zimm, B. H. *J. Chem. Phys.* **1948**, *16*, 1099.
(29) Wyatt, P. J. *Anal. Chim. Acta* **1993**, *272*, 1.
(30) Kratochvíl, P. *Classical Light Scattering from Polymer Solutions;* Jenkins, A. D., Ed.; Elsevier Science Publishers: New York, 1987.
(31) Brandup, J., Immergut, E. H., Eds. *Polymer Handbook*, 3rd ed.; John Wiley and Sons: New York, 1989.

(32) Stejskal, J.; Konák, C.; Helmstedt, M.; Kratochvíl, P. *Collect. Czech. Chem. Commun.* **1993**, *58*, 2282.
(33) Adam, M. *Macromolecules* **1977**, *10*, 1229.
(34) de Gennes, P.-G. *Scaling Concepts in Polymer Physics*; Cornell University Press: Ithaca, NY, 1979.
(35) O'Driscoll, K.; Sanayei, R. A. *Macromolecules* **1991**, *24*, 4479.
(36) Morcellet, M.; Louceux, C. *Makromol. Chem.* **1978**, *179*, 2439.
(37) Zhou, Z.; Chu, B. *J. Colloid Interface Sci.* **1988**, *126*, 171.
(38) Price, C.; McAdam, J. D. G.; Lally, T. P.; Woods, D. *Polymer* **1974**, *15*, 228.
(39) Orofino, T. A.; Flory, P. J. *J. Phys. Chem.* **1959**, *63*, 283.
(40) Kitano, T.; Taguchi, A.; Noda, I.; Nagasawa, M. *Macromolecules* **1980**, *13*, 57.
(41) Kato, T.; Tokuya, T.; Nozaki, T.; Takahashi, A. *Polymer* **1984**, *25*, 218.
(42) (a) Tian, M.; Qin, A.; Ramireddy, C.; Webber S. E.; Munk, P.; Tuzar, Z.; Prochazka, K. *Langmuir* **1993**, *9*, 1741. (b) Tuzar, Z.; Kratochvil, P.; Prochazka, K.; Munk, P. *Collect. Czech. Chem. Commun.* **1993**, *58*, 2362.
(43) Nguyen, D.; Zhong, X.-F.; Williams, C. E.; Eisenberg, A. *Macromolecules* **1994**, *27*, 5173.
(44) Nagasawa, M.; Takahashi, A. In *Light Scattering from Polymer Solutions*; Huglin, M. B., Ed.; Academic Press: New York, 1972; Chapter 16.
(45) Takahashi, A.; Hayashi, J.; Kagawa, I. *Kogyo Kagaku Zasshi* **1957**, *60*, 1059.
(46) Stejskal, J.; Benes, M. J.; Kratochvíl, P.; Peska, J. *J. Polym. Sci.* **1973**, *11*, 1803.
(47) Buscall, R. *J. Chem. Soc., Faraday Trans. 1* **1981**, *77*, 909.
(48) Barlow, R. J.; Zimmerman, S.: Khougaz, K.; Eisenberg, A. Submitted for publication in *J. Polym. Sci., Polym. Phys. Ed.*
(49) Xu, R.; Winnik, M. A.; Hallett, F. R.; Riess, G.; Croucher, M. D. *Macromolecules* **1991**, *24*, 87.
(50) Zhang, L.; Barlow, R. J.; Eisenberg, A. *Macromolecules*, in press.
(51) Gao, Z.; Varshney, S. K.; Wong, S.; Eisenberg, A. *Macromolecules* **1994**, *26*, 7923.
(52) Nguyen, D.; Williams, C. E.; Eisenberg, A. Submitted for publication in *Macromolecules*.
(53) Flory, P. J. *Principles of Polymer Chemistry;* Cornell University Press: New York, 1953; Chapter 12, p 530.
(54) Cogan, K. A.; Gast, A. P.; Capel, M. *Macromolecules* **1991**, *24*, 6512.
(55) Nguyen, D.; Varshney, S. K.; Williams, C. E.; Eisenberg, A. *Macromolecules* **1994**, *27*, 5086.
(56) Soen, T.; Inoue, T.; Miyoshi, K.; Kawai, H. *J. Polym. Sci., Polym. Phys. Ed.*, **1972**, *10*, 757.
(57) Polik, W. F.; Burchard, W. *Macromolecules* **1983**, *16*, 978.
(58) Polverari, M.; van de Ven, T. G. M. To be published in *J. Solution Chem.*

MA950037H